DOI 10.1007/s10778-024-01253-1
International Applied Mechanics, Vol. 59, No. 6, November, 2023

NONSTATIONARY VIBRATIONS OF A VISCOELASTIC FUNCTIONALLY GRADED CYLINDER

I. V. Yanchevskyi[1*] and L. O. Hryhorieva[2]**

A unified approach to the analysis of the nonstationary vibrations of piezoelectric ceramic plane layers, cylinders, and spheres taking into account the functional inhomogeneity and viscoelasticity of the material is proposed. The standard model of vibration damping and the Kelvin–Voigt viscoelastic model are considered. The proposed approach makes it possible to study the transition of the transducer to a static state or to a steady-state vibration mode under nonstationary perturbations. The effect of functional inhomogeneity on the nonstationary vibrations of a piezoelectric element is analyzed. The damping of the vibrations and viscoelastic axisymmetric vibrations of a radially polarized cylinder under electrical and mechanical perturbation using the Heaviside function is calculated. The dynamics of damping is analyzed, and the obtained results are compared with the static solution to validate the results. The generation of voltage by a piezoceramic cylinder under mechanical axisymmetric loading is also studied taking into account the viscoelastic properties of the material. It was found that the time to reach the steady-state mode for mechanical and electrical loads is almost the same.

Keywords: nonstationary electroelasticity, piezoceramic cylinder, functionally graded material, energy dissipation, vibration damping, Voigt viscoelastic model

Introduction. The vibrations of piezoelectric transducers under nonstationary electrical and mechanical perturbations in the electroelastic statement were considered in [1, 5, 11, 12, 17, etc.]. The results obtained may differ from the actual values due to the manifestation of the viscoelastic properties of piezoelectrics and material inhomogeneity. In the physical context, nonstationary perturbations damp over time and change over to steady-state vibrations or static state, depending on the type of load. The process of piezoelectric bodies' reaching the steady mode under nonstationary perturbations has not been studied well.

Steady-state vibrations of piezoelectric bodies were widely described using a linear problem statement [2–4, 6, 7, 10, 13–16, etc.]. In particular, [6, 9, 15] describe modern methods and approaches to analyzing the dynamic behavior of electrically elastic bodies, their interaction with acoustic and thermal fields, and working standards for determining material characteristics. The main types, geometry, operating modes, and operating features of the most common piezoelectric elements are described in [3].

Piezoelectric transducers can operate both in the generation mode (inverse piezoelectric effect, actuator) and in the mode of receiving vibrations (direct piezoelectric effect, sensor) [3–6]. In the latter case, a potential difference occurs on the open electrodes, i.e., an electrical signal is generated that can be read by other devices in the electrical circuit. The problem of identifying the input mechanical signal from the output electrical signal for bimorphic bodies was solved in [5].

For steady-state vibrations, a common way to take into account energy damping is to introduce material characteristics in a complex form. In this approach, the main problem is to obtain a complete set of loss tangents for the mechanical, electrical, and dielectric characteristics of the material (10 constants total), which, in the general case, depend on the frequency range of the

[1]National Technical University of Ukraine "Igor Sikorsky Kyiv Polytechnic Institute," 37 Beresteiskyi Av., Kyiv, Ukraine, 03056; *e-mail: i.yanchevskyi@kpi.ua. [2]Kyiv National University of Construction and Architecture, 31 Povitroflotskyi Ave., Kyiv, Ukraine, 01063; **e-mail: l_grigoryeva@ukr.net. Translated from Prykladna Mekhanika, Vol. 59, No. 6, pp. 84–94, November–December 2023. Original article submitted January 28, 2023.

load [16]. Taking into account the energy dissipation with the help of complex moduli makes it possible to find the real amplitude values of the parameters of the electromechanical state of the transducer in the vicinity of resonances [4]. In the interresonance range, energy dissipation has little effect on vibrations, and the calculation with real material constants provides a satisfactory result. Dissipative heating of piezoelectric viscoelastic layered shells was studied using a nonlinear problem statement in [2, 13].

The problem of discrepancy between the real electromechanical state and the mathematical model can also be related to the inhomogeneity of material characteristics. Functional inhomogeneity of the material can be specially designed and implemented to ensure special energy conversion tasks. Functionally graded materials are obtained by combining materials with different values of physical and chemical parameters. Functionally graded piezoelectric cells are used for sensors, actuators, and energy harvesters since the appropriate arrangement can eliminate the disadvantages of traditional materials and enhance the benefits of the materials used. The forced vibrations of multilayer and functionally graded piezoceramic cylinders are studied in [10] by the method of separation of variables using spline collocations and the method of discrete orthogonalization. The method of separation of variables in the coordinates x, y is used for rectangular plates in [14]. Functionally inhomogeneous piezoceramic plates, cylinders, and spheres under static loads were designed in [8, 18].

One of the simplest methods for taking into account vibration damping is to introduce a damping element proportional to the displacement rate into the equation of motion. This model of damping directly follows from the law of energy conservation and is equally suitable for both nonstationary mode and harmonic analysis [7, 13].

The viscoelastic Voigt (or Kelvin–Voigt) model can be implemented exclusively by a viscous damper (Newtonian viscous body) and a purely elastic element (Hookean elastic body) connected in parallel. This model qualitatively describes the phenomenon of elastic aftereffect, in which the deformation develops with a delay relative to the applied load [7, 13]. Thus, the damping element is introduced into the material relations and is proportional to the strain rate [7].

In this paper, a new approach to analyzing the nonstationary vibrations of functionally inhomogeneous viscoelastic piezoceramic bodies is proposed, based on the universal approach to studying vibrations of plane layers, cylinders, and spheres described in [1, 12].

1. Simplest Model of Vibration Damping. We consider the thickness vibrations of a plane piezoelectric element or axisymmetric vibrations of a hollow sphere and an infinite cylinder with consideration of the functionally graded and viscoelastic properties of the material. To study them, we use the generalized approach used in [1, 12] with the introduction of the parameter N, where $N = 0$ corresponds to a plane piezoelectric element; $N = 1$ corresponds to a cylindrical, $N = 2$ corresponds to a spherical body. The following notation is used in the problem statement: radial r (for a plane layer, thickness) coordinate; electric displacement D_r in the direction of the axis r; σ_{rr}, $\sigma_{\theta\theta}$ are the radial (thickness) and circumferential (transverse) mechanical stresses; electric potential φ; elastic moduli c_{ij}^E at constant electric field; piezoelectric moduli e_{ij}; dielectric constant ε_{ij}^S at constant strain. All the material characteristics are considered to be functionally dependent on the thickness coordinate:

$$\rho = \rho(r), \qquad c_*^E = c_*^E(r), \qquad e_* = e_*(r), \qquad \varepsilon_{33}^S = \varepsilon_{33}^S(r).$$

Hereinafter, R_1, R_2 are the inner and outer radii of the cylinder or sphere; h is the wall thickness of the piezoelectric element.

All subsequent formulas and results will be represented in dimensionless form:

$$\bar r = \frac{r}{h}, \quad \bar t = \frac{t}{t_h}, \quad \bar u = \frac{u}{h}, \quad \bar\sigma_* = \frac{\sigma_*}{c_{00}}, \quad \bar\varphi = \frac{\varphi}{h}\sqrt{\frac{\varepsilon_{33}^S}{c_{00}}}, \quad \bar D_r = \frac{D_r}{\sqrt{c_{00}\varepsilon_{33}^S}},$$

$$\bar\rho = \frac{\rho}{\rho_{00}}, \quad \bar c_* = \frac{c_*^E}{c_{00}}, \quad \bar k_1 = \frac{k_1 h^2}{c_{00} t_h}, \quad \bar e_* = \frac{e_*}{\sqrt{c_{00}\varepsilon_{33}^S}}, \quad \bar\varepsilon_{33} = 1, \tag{1.1}$$

where $t_h = h\sqrt{\rho_{00}/c_{00}}$, $c_{00} = c_{33}^E + e_{33}^2/\varepsilon_{33}^S$, $\rho_{00} = \rho$.

Tabulated values of material characteristics are used for normalizing values.

Dependences (1.1) are chosen so that the input equations do not change their form. We omit the dimensionless signs below.

The simplest model of vibration damping is formed by introducing a damping term into the equation of motion in the form of the product of rate and damping coefficient k_1

$$\frac{\partial \sigma_{rr}}{\partial r} + \frac{N}{r}(\sigma_{rr} - \sigma_{\theta\theta}) = \rho \frac{\partial^2 u}{\partial t^2} + k_1 \frac{\partial u}{\partial t}. \tag{1.2}$$

Maxwell's quasistatic equation in this model has the classical form

$$\frac{\partial D_r}{\partial r} + \frac{N}{r} D_r = 0. \tag{1.3}$$

The material relations for thickness polarization are written as follows [1]:

$$\sigma_{rr} = c_{33}^E \frac{\partial u}{\partial r} + N c_{13}^E \frac{u}{r} + e_{33} \frac{\partial \varphi}{\partial r},$$

$$\sigma_{\theta\theta} = c_{13}^E \frac{\partial u}{\partial r} + N\left(c_{11}^E - \frac{1}{2}(N-1)(c_{11}^E - c_{13}^E)\right)\frac{u}{r} + e_{13} \frac{\partial \varphi}{\partial r},$$

$$D_r = e_{33} \frac{\partial u}{\partial r} + N e_{31} \frac{u}{r} - \varepsilon_{33}^S \frac{\partial \varphi}{\partial r}. \tag{1.4}$$

Substitute (1.4) into (1.2), (1.3), taking into account the functional dependence of the material constants on the coordinate *r*. The dash next to the material characteristic indicates the derivative with respect to the thickness coordinate:

$$\rho \frac{\partial^2 u}{\partial t^2} + k_1 \frac{\partial u}{\partial t} = c_{33} \frac{\partial^2 u}{\partial r^2} + \left(c'_{33} + N \frac{c_{33}}{r}\right)\frac{\partial u}{\partial r} + \left(N \frac{c'_{13}}{r} - N \frac{c_{13}}{r^2} + N^2 \frac{c_{13} - a}{r^2}\right)u$$

$$+ e_{33} \frac{\partial^2 \varphi}{\partial r^2} + \left(e'_{33} + N \frac{e_{33} - e_{31}}{r}\right)\frac{\partial \varphi}{\partial r}, \tag{1.5}$$

$$e_{33} \frac{\partial^2 u}{\partial r^2} + \left(e'_{33} + N \frac{e_{13} + e_{33}}{r}\right)\frac{\partial u}{\partial r} + \left(N \frac{e'_{31}}{r} + N(N-1)\frac{e_{13}}{r^2}\right)u$$

$$- \varepsilon_{33} \frac{\partial^2 \varphi}{\partial r^2} - \left(\varepsilon'_{33} + N \frac{\varepsilon_{33}}{r}\right)\frac{\partial \varphi}{\partial r} = 0. \tag{1.6}$$

In (1.5), the replacement $a = c_{11} - (N-1)(c_{11} - c_{13})/2$ is used.

Equations (1.5), (1.6) are supplemented with mechanical boundary conditions

$$u(R_{,t}) = U_i(t) \quad \text{or} \quad \sigma_{rr}(R_{,t}) = P_i(t) \quad (i = 1, 2), \tag{1.7}$$

boundary conditions for electric field quantities

$$\varphi(R_1) = 0, \qquad \varphi(R_2) = V(t) \tag{1.8}$$

and initial conditions

$$u|_{t=0} = U_0(r), \qquad \left.\frac{du}{dt}\right|_{t=0} = W_0(r). \tag{1.9}$$

In (1.5) and (1.6), we move from a continuum to a discrete statement in a spatial coordinate using finite-difference expressions of the second order of accuracy. We introduce the partition $r_i = R_1 + (i-1)\Delta$ ($\Delta = h/m$, $i = 1, \ldots, m+1$) and look for a solution with respect to $u_i = u(r_i)$ and $\varphi_i = \varphi(r_i)$. We get a system of equations that can be written in matrix form as follows:

$$\rho \frac{\partial^2 \mathbf{u}}{\partial t^2} + k_1 \frac{\partial \mathbf{u}}{\partial t} = \mathbf{A}\mathbf{u} + \mathbf{B}\varphi, \tag{1.10}$$

$$\mathbf{C}\mathbf{u} + \mathbf{D}\varphi = 0. \tag{1.11}$$

To solve the system of equations (1.10), (1.11), an implicit time integration scheme is used. We use the Newmark scheme (here ξ is the parameter of the scheme; Δt is the time step; u^{p+1}, $\dot{u}^{p+1}$, $\ddot{u}^{p+1}$ are displacements, velocities and accelerations at the moment of time $t^{p+1} = p\Delta t$):

$$\dot{u}^{p+1} = \frac{u^{p+1} - u^p}{\xi \Delta t} - \frac{1-\xi}{\xi} \dot{u}^p, \qquad \ddot{u}^{p+1} = \frac{u^{p+1} - u^p}{\xi^2 \Delta t^2} - \frac{1}{\xi^2 \Delta t} \dot{u}^p - \frac{1-\xi}{\xi} \ddot{u}^p. \tag{1.12}$$

Substituting (1.12) into (1.10), we obtain the system of equations

$$\left(\frac{\rho}{\xi^2 \Delta t^2} + \frac{k_1}{\xi \Delta t} \right) \mathbf{u}^{p+1} - \mathbf{A}\mathbf{u}^{p+1} - \mathbf{B}\varphi^{p+1}$$

$$= \left(\frac{\rho}{\xi^2 \Delta t^2} + \frac{k_1}{\xi \Delta t} \right) \mathbf{u}^p + \left(\frac{\rho}{\xi^2 \Delta t} + k_1 \frac{1-\xi}{\xi} \right) \dot{\mathbf{u}}^p + \rho \frac{1-\xi}{\xi} \ddot{\mathbf{u}}^p,$$

$$\mathbf{C}\mathbf{u}^{p+1} + \mathbf{D}\varphi^{p+1} = 0. \tag{1.13}$$

System (1.13) is supplemented with the boundary conditions (1.7), (1.8) using (if necessary) one-sided difference expressions

$$\left. \frac{df}{dx} \right|_i = \frac{3f_i - 4f_{i-1} + f_{i-2}}{2\Delta}, \qquad \left. \frac{df}{dx} \right|_i = \frac{-3f_i + 4f_{i+1} - f_{i+2}}{2\Delta}. \tag{1.14}$$

When a piezoelectric device operates in the direct piezoelectric effect mode, the potential difference across its open electrodes is determined by displacement using the following mathematical transformations of Maxwell's equation [5]:

$$rD_r = r\left(e_{33} \frac{\partial u}{\partial r} + Ne_{31} \frac{u}{r} - \varepsilon_{33}^S \frac{\partial \varphi}{\partial r} \right) = \text{const} = 0,$$

$$Ne_{31} \frac{u}{r} = \varepsilon_{33}^S \frac{\partial \varphi}{\partial r} - e_{33} \frac{\partial u}{\partial r}, \qquad Ne_{31} \int_{R_1}^{R_2} \frac{u}{r} dr = \int_{R_1}^{R_2} \left(\varepsilon_{33}^S \frac{\partial \varphi}{\partial r} - e_{33} \frac{\partial u}{\partial r} \right) dr,$$

$$Ne_{31} \int_{R_1}^{R_2} \frac{u}{r} dr = \varepsilon_{33}^S \left(\varphi|_{r=R_2} - \varphi|_{r=R_1} \right) - e_{33} \left(u|_{r=R_2} - u|_{r=R_1} \right).$$

When changing over from continuous to discrete expressions, we have

$$V = \varphi_{m+1} - \varphi_1 = \frac{e_{33}}{\varepsilon_{33}^S} (u_{m+1} - u_1) + \frac{Ne_{31}}{\varepsilon_{33}^S} \sum_{=1}^{m} \frac{u_i}{r_i} \Delta. \tag{1.15}$$

Taking into account the functional inhomogeneity of the material, we transform (1.15) to the form

$$e_{33}(R_2) u_{m+1} - e_{33}(R_1) u_1 - [\varepsilon_{33}^S(R_2) \varphi_{m+1} - \varepsilon_{33}^S(R_1) \varphi_1]$$
$$+ \sum_{i=1}^{m} \left(-e'_{33}(r_i) u_i + \varepsilon'_{33}(r_i) \varphi_i + Ne_{31}(r_i) \frac{u_i}{r_i} \right) \Delta = 0. \tag{1.16}$$

Equation (1.15) or (1.16) is used as an electrical boundary condition when the element is mechanically loaded and describes the relationship between the generated voltage and the displacements of the element.

2. Kelvin–Voigt Model. In the Kelvin–Voigt damping model, the equations of motion and Maxwell's equation have the classical form:

$$\frac{\partial \sigma_{rr}}{\partial r} + \frac{N}{r}(\sigma_{rr} - \sigma_{\theta\theta}) = \rho \frac{\partial^2 u_r}{\partial t^2}, \tag{2.1}$$

$$\frac{\partial D_r}{\partial r} + \frac{N}{r} D_r = 0. \tag{2.2}$$

The damping terms in the stress expressions are proportional to the strain rate. Since in the axisymmetric case, the expressions include two linear strains (ε_{rr}, $\varepsilon_{\theta\theta}$) and two normal stresses (σ_{rr}, $\sigma_{\theta\theta}$), we introduce three damping coefficients k_{33}, k_{13}, and k_{11} with indexing corresponding to the indices of the elastic moduli c_{ij}^E. To avoid stress coupling in the plane case, the circumferential strain rate is multiplied by N:

$$\sigma_{rr} = c_{33}^E \varepsilon_{rr} + N c_{13}^E \varepsilon_{\theta\theta} - e_{33} E_r + k_{33} \dot{\varepsilon}_{rr} + k_{13} N \dot{\varepsilon}_{\theta\theta},$$

$$\sigma_{\theta\theta} = c_{13}^E \varepsilon_{rr} + N a \varepsilon_{\theta\theta} - e_{13} E_r + k_{13} \dot{\varepsilon}_{rr} + k_{11} N \dot{\varepsilon}_{\theta\theta},$$

$$D_r = e_{33} \varepsilon_{xx} + N e_{31} \varepsilon_{\theta\theta} + \varepsilon_{33}^S E_r, \quad \varepsilon_{rr} = \frac{\partial u}{\partial r}, \quad \varepsilon_{\theta\theta} = \frac{u}{r}, \quad E_r = -\frac{\partial \varphi}{\partial r}. \tag{2.3}$$

We assume that the damping coefficients are proportional to the corresponding coefficients of Eqs. (2.3):

$$\frac{k_{33}}{k_{13}} = \frac{c_{33}^E}{c_{13}^E}, \quad \frac{k_{13}}{k_{11}} = \frac{c_{13}^E}{a}.$$

Problems (2.1)–(2.3) are supplemented with the boundary and initial conditions (1.7)–(1.9).

With the introduction of the velocity v as an additional unknown function, it is convenient to change over from system (2.1), (2.2) to a system of ordinary differential equations of the first order and apply standard methods (e.g., the Runge–Kutta method) for time integration. Substituting (2.3) into (2.1), we get

$$\frac{\partial u}{\partial t} = v, \quad \frac{\partial v}{\partial t} = \left[c_{33}^E \frac{\partial^2 u}{\partial r^2} + \left(c'_{33} + \frac{N}{r} c_{33}^E \right) \frac{\partial u}{\partial r} + \left(\frac{N c'_{13}}{r} - \frac{N^2}{r^2} a \right) u + e_{33} \frac{\partial^2 \varphi}{\partial r^2} \right.$$

$$\left. + \left(e'_{33} + \frac{N}{r}(e_{33} - e_{13}) \right) \frac{\partial \varphi}{\partial r} + k_{33} \frac{\partial^2 v}{\partial r^2} + \frac{k_{33} N}{r} \frac{\partial v}{\partial r} + \frac{N}{r^2}(N(k_{13} - k_{11}) - k_{13}) v \right] \Big/ \rho. \tag{2.4}$$

Equation (2.4) is supplemented with Maxwell's equation in the form (1.6) and the boundary conditions

$$\sigma_{rr} = \left(c_{33}^E \frac{\partial u}{\partial r} + N c_{13}^E \frac{u}{r} + e_{33} \frac{\partial \varphi}{\partial r} + k_{33} \frac{\partial v}{\partial r} + k_{13} N \frac{v}{r} \right)_{r=R_i} = P_i(t) \quad (i = 1, 2). \tag{2.5}$$

The electrical boundary conditions are chosen in the form (1.8).

We look for a solution in the form of the vector

$$\mathbf{Y} = \{u_1, \ldots, u_{m+1}, v_1, \ldots, v_{m+1}, \varphi_1, \ldots, \varphi_{m+1}\}, \tag{2.6}$$

where u_i, v_i, φ_i are the displacement, velocity, and electric potential at the $r_i = R_1 + (i-1)\Delta$ ($\Delta = h/m$, $i = 1, \ldots, m+1$) partition points.

TABLE

c_{11}^E	c_{12}^E	c_{13}^E	c_{33}^E	c_{44}^E	e_{13}	e_{33}	e_{15}	ε_{11}^S	ε_{33}^S	ρ
10^{10} Pa					C/m^2			ε_0		kg/m^3
13.9	7.78	7.43	11.5	2.56	–5.2	15.1	12.7	730	635	7500

From the difference form of Eq. (1.6) in matrix form (1.11), we express the electric potential in terms of displacement and differentiate it with respect to time:

$$\varphi = -\mathbf{D}^{-1}\mathbf{C}\mathbf{u} \to \dot{\varphi} = -\mathbf{D}^{-1}\mathbf{C}\mathbf{v}. \tag{2.7}$$

We differentiate (2.5), (1.8) with respect to time and supplement the system of equations with expressions for the unknown quantities at the edge points

$$\frac{\partial u_1}{\partial t} = v_1, \qquad \frac{\partial u_{m+1}}{\partial t} = v_{m+1},$$

$$\frac{\partial v_1}{\partial t} = \left[\frac{c_{33}^E}{2\Delta r}(-3v_1 + 4v_2 - v_3) + Nc_{13}^E\frac{v_1}{R_0} + \frac{e_{33}}{2\Delta r}\left(-3\frac{\partial\varphi_1}{\partial t} + 4\frac{\partial\varphi_4}{\partial t} - \frac{\partial\varphi_3}{\partial t}\right)\right.$$

$$\left. + \frac{k_{33}}{2\Delta r}\left(4\frac{\partial v_2}{\partial t} - \frac{\partial v_3}{\partial t}\right)\right] \Big/ \left(\frac{3k_{33}}{2\Delta r} - \frac{k_{13}N}{R_0}\right),$$

$$\frac{\partial v_{m+1}}{\partial t} = -\left[\frac{c_{33}^E}{2\Delta r}(3v_{m+1} - 4v_m + v_{m-1}) + Nc_{13}^E\frac{v_{m+1}}{R_1} + \frac{e_{33}}{2\Delta r}\left(3\frac{\partial\varphi_{m+1}}{\partial t} - 4\frac{\partial\varphi_m}{\partial t} + \frac{\partial\varphi_{m-1}}{\partial t}\right)\right.$$

$$\left. + \frac{k_{33}}{2\Delta r}\left(-4\frac{\partial v_m}{\partial t} + \frac{\partial v_{m-1}}{\partial t}\right) - P_1\right] \Big/ \left(\frac{3k_{33}}{2\Delta r} + \frac{k_{13}N}{R_1}\right),$$

$$\frac{\partial\varphi_1}{\partial t} = 0, \qquad \frac{\partial\varphi_{m+1}}{\partial t} = \dot{V}. \tag{2.8}$$

System (2.4), (2.6)–(2.8) is written in the form

$$\dot{\mathbf{Y}} = \mathbf{F}\mathbf{Y}. \tag{2.9}$$

The system of differential equations (2.8) is solved by the Runge–Kutta method under the initial conditions

$$\mathbf{u}|_{t=0} = U_0(\mathbf{r}), \qquad \mathbf{v}|_{t=0} = W_0(\mathbf{r}), \qquad \varphi|_{t=0} = -\mathbf{D}^{-1}\mathbf{C}U_0(\mathbf{r}), \qquad \mathbf{r} = (r_1, \ldots, r_{m+1}). \tag{2.10}$$

3. Numerical Results. Let us consider piezoceramic hollow radially polarized cylinders ($N = 1$) made of PZT-4 piezoceramics or a functionally graded material based on PZT-4 (table).

It is assumed that the cylindrical surfaces are free of mechanical loads ($P_1 = P_2 = 0$), and a stepwise unit electric signal is applied to the conductive coatings of the piezoelectric elements ($V(t) = H(t)$, $H(t)$ is the Heaviside function). The geometry of the piezoelectric elements is determined by the dimensionless parameters R_1 and R_2.

When modeling the functional inhomogeneity of the material characteristics, it was assumed that their thickness distribution is parabolic with a factor

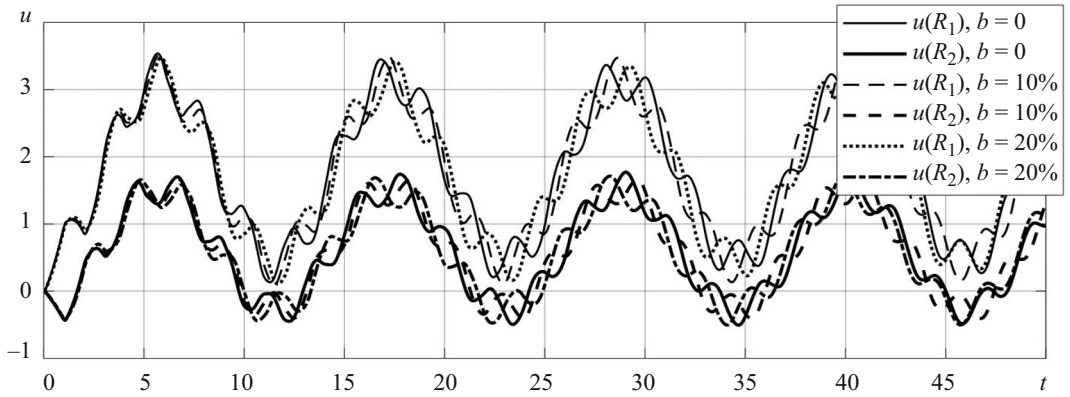

Fig. 1

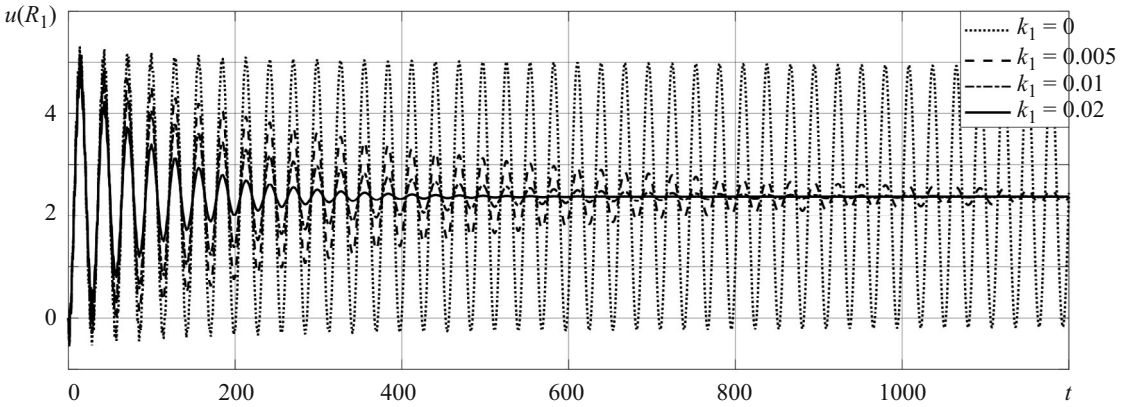

a

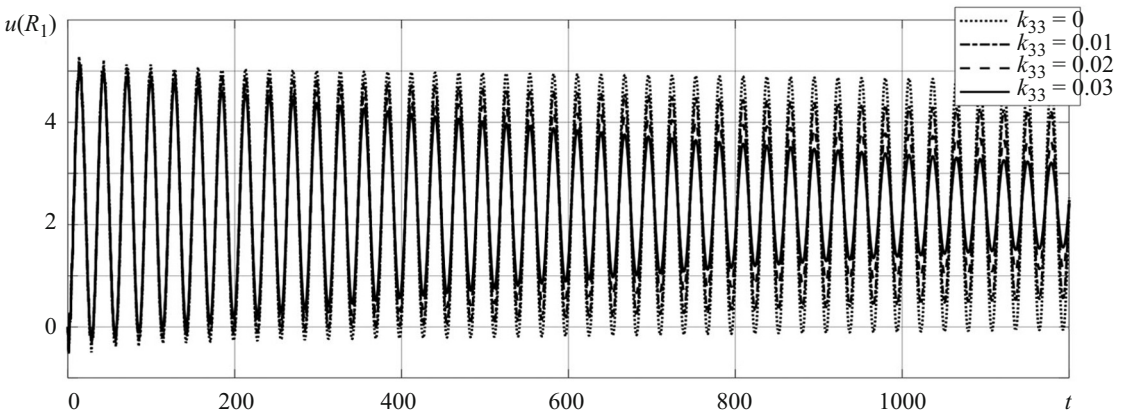

b

Fig. 2

$$f(r)=\frac{4b}{h^2}\left(x-\frac{h}{2}\right)^2+1-b, \tag{3.1}$$

where b is the deviation of the material characteristic from the tabulated values on the central fibers in percent; $x=r-R_1$ is the thickness coordinate.

Figure 1 shows the vibration curves of the outer surfaces of the cylinder with radii $R_1=1$ and $R_2=2$. When $b=0$ we have an inhomogeneous cylinder material, and when $b=10\%$ and 20% all the material characteristics from the table change as in (3.1) relative to the tabulated values.

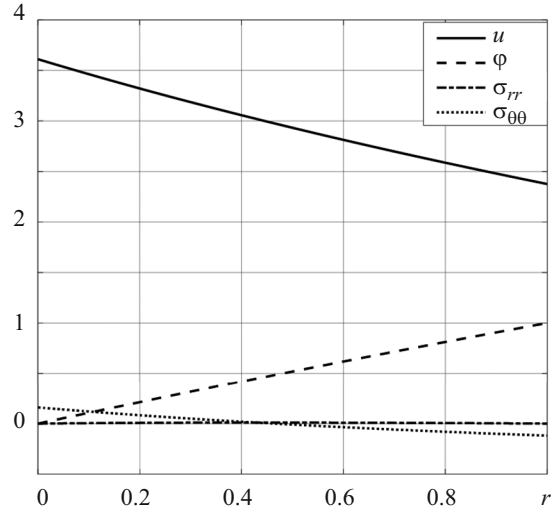

Fig. 3

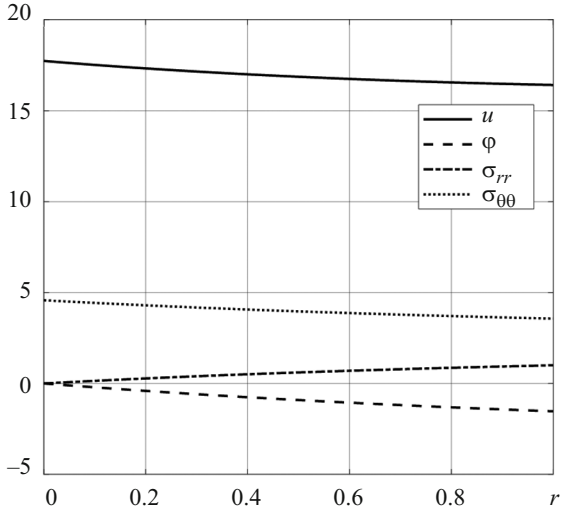

Fig. 4

Figure 1 shows that functional inhomogeneity affects only the propagation rate of thickness vibrations. In this case, due to the decrease in the material characteristics relative to the homogeneous body, the propagation velocity decreases, which is consistent with the results in [1, 11]. The vibration amplitude of the cylinder midsurface does not depend on *b*, and the period increases by 0.4% per every 10% deviation.

Figure 2 compares the damping models. Figure 2*a* shows the nonstationary vibrations of the outer surface of a homogeneous cylinder with radii $R_1 = 3$ and $R_2 = 4$ for models (1.2)–(1.4) and different values of the damping coefficient k_1. We see that when $k_1 = 0.02$, almost complete damping occurs when $t_з = 500$; when $k_1 = 0.01$—$t_з = 900$, and when $k_1 = 0.005$—$t_з = 1500$. The dimensionless unit of time for a body with a wall thickness of 1 cm corresponds to $2.2 \cdot 10^{-6}$ sec, i.e., the damping times are 1.1 msec, 1.98 msec, and 3.3 msec, respectively. The vibrations of a viscoelastic body approach the solution of the corresponding static problem (Fig. 2) $u(R_2) = 2.4$, with the amplitude decreasing exponentially.

Figure 2*b* show the vibrations of the outer surface of the same cylinder according to the viscoelastic Voigt model (2.1)–(2.3) for different values of the damping coefficient k_{33}.

We can see that the amplitude decreases, approaching to the static solution. During the observation period (2.64 msec), the amplitude of vibrations decreased by 30% when $k_{33} = 0.01$; by 53% when $k_{33} = 0.02$, and by 67% when $k_{33} = 0.03$. There are 42 vibration cycles in the interval under consideration. Thus, it can be predicted that when $k_{33} = 0.03$, beginning from $t_з = 2200$, the deviation from the static value will not exceed 3%. The period of vibrations is $61.6 \cdot 10^{-6}$ sec, and the frequency is 16.2 Hz.

Figure 3 shows the results for the cylinder loaded with a unit potential difference in the static case.

The displacement is 3.6 on the inner surface and 2.37 on the outer surface. That is, from in Figs. 2 and 3, it follows that, the viscoelastic properties of the material are taken into account, the electroelastic vibrations tend to the static solution, which is fully consistent with the classical vibration theory and indicative of the correctness of the results obtained.

The generation of voltage under mechanical loading of the piezoceramic cylinder illustrates the direct piezoelectric effect. Figure 4 shows the calculated for a unit external pressure $P_2 = 1$ in the static case. The displacements change from 17.74 on the inner surface to 16.42 on the outer surface. The difference in electrical potential is 1.53.

Figure 5 shows the curves of dynamic displacements of the outer surface of the cylinder and the generated voltage between its open electrodes. Here model (1.2)–(1.4) for $P_1 = 0$, $P_2 = H(t)$ and the electrical boundary condition (1.15) are used.

Figure 5 shows pulsating vibrations of the outer surface. The damping with the values of k_1 considered is the same as in Fig. 2*a*. The displacements tend to $u(R_2) = 16.4$, and the electric potential to $\varphi(R_2) = -1.52$, which is fully consistent with the results in Fig. 4.

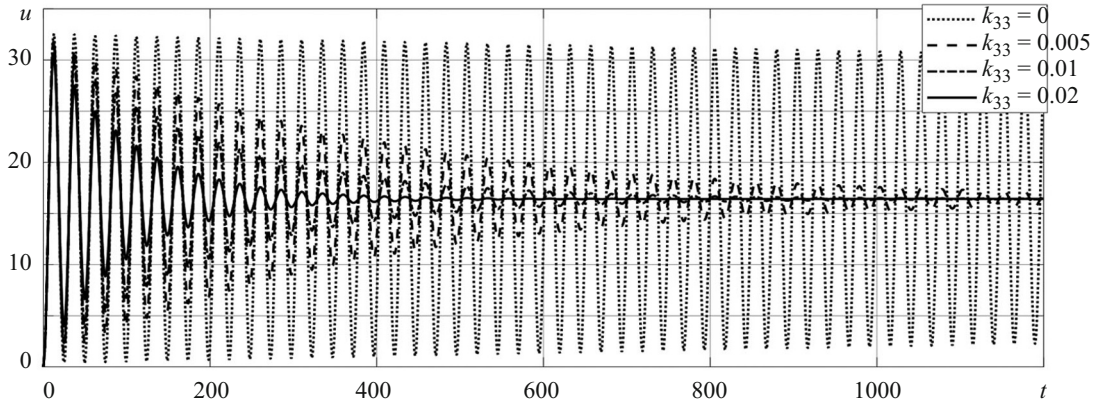

a

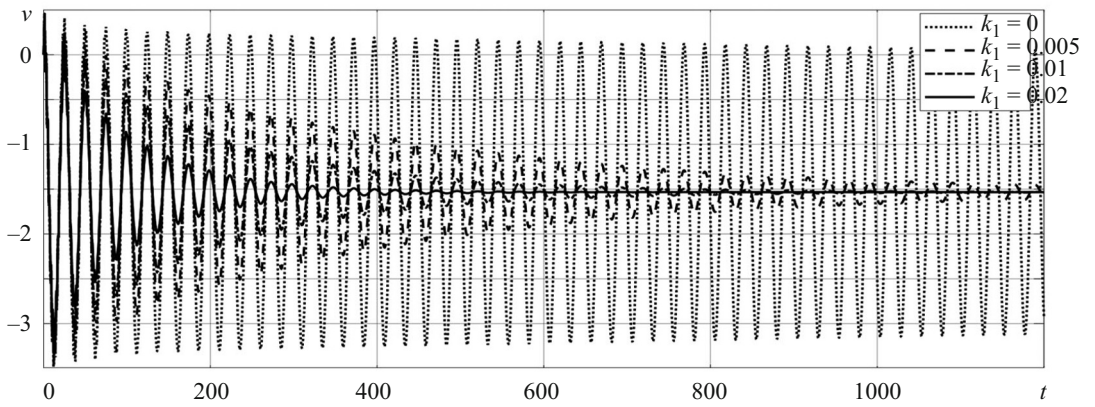

b

Fig. 5

The period of mechanically caused vibrations is about 12% shorter than under electrical load. Vibration frequency is 18.5 kHz. The amplitude decreases nonlinearly. The maximum displacements that occur under the step loading are twice as high as those in the static case. The same is true for mechanical stresses.

Conclusions. A numerical solution to the problem of the nonstationary vibrations of a radially polarized viscoelastic piezoceramic cylinder made of a functionally graded material has been obtained. The effect of the functional inhomogeneity of the material is manifested as a change in the propagation rate of perturbations along the thickness. Comparing two models of energy dissipation, it was found that the inclusion of a damping element proportional to the displacement rate in the equation of motion causes damping much faster than in the Voigt model with the same damping coefficients. Numerical calculations have shown that the perturbations caused by a nonstationary load have a vibration amplitude that is approximately twice as high as the corresponding value in the static case. To determine the damping coefficients using both methods, it is necessary to know the damping time in a real object. In general, the two models of energy dissipation have similar vibrations, i.e., the simpler one can be used in the future.

During the study of voltage generation under mechanical load, the vibration frequency increased. With a positive external load, the displacements occur in a positive region, and the potential difference is negative. The displacement and electric potential curves are proportional to each other at the scale considered.

The results obtained are important for assessing the electromechanical state, including the electrical and mechanical strength of the piezoelectric element under nonstationary perturbations. The proposed approach makes it possible to analyze transient modes for piezoceramic planar bodies, cylinders, and spheres, including those made of functionally graded material.

REFERENCES

1. L. O. Hryhorieva and I. V. Yanchevskyi, "Nonstationary vibrations of piezoelectric transducers made of functionally graded materials," *Probl. Obch. Mekh. Mits. Konstr.*, No. 35, 29–41 (2022).
2. I. F. Kirichok, Y. A. Zhuk, and T. V. Karnaukhova, "Damping of the resonant axisymmetric vibration of an infinitely long viscoelastic cylindrical shell containing piezoelectric sensor and actuator, with allowance for self-heating," *Visn. Kyiv. Nats. Univ. im. Tarasa Shevchenka*, No. 1, 35–40 (2015).
3. V. M. Sharapov, J. V. Sotula, and L. G. Kunitskaya, *Electroacoustic Transducers*, Tekhnosfera, Moscow (2013).
4. M. O. Shul'ga and V. L. Karlash, *Resonant Electromechanical Vibrations of Piezoelectric Plates* [in Ukrainian], Naukova Dumka, Kyiv (2008).
5. I. V. Yanchevskyi, *Nonstationary Vibrations of Bimorphic Electrically Elastic Bodies*, KPI im. Igorya Sikorskogo, Kyiv (2023).
6. I. J. Busch-Vishniac, *Electromechanical Sensors and Actuators*, Springer, New York (1999).
7. C. F. Chazal and R. Moutou Pitti, "An incremental constitutive law for ageing viscoelastic materials: a three-dimensional approach," *Compt. Rend. Mécan.*, **337**, No. 1, 30–33 (2009).
8. H. L. Dai, Y. M. Fu, and J. H. Yang, "Electromagnetoelastic behaviors of functionally graded piezoelectric solid cylinder and sphere," *Acta Mech. Sinica*, **23**, No. 1, 55–63 (2007).
9. D. Fang, F. Li, B. Liu, and Y. Zhang, "Advances in developing electromechanically coupled computational methods for piezoelectrics/ferroelectrics at multiscale," *Appl. Mech. Reviews*, **65**, No. 6, 52 (2013).
10. A. Y. Grigorenko, W. H. Müller, and I. A. Loza, *Selected Problems in the Elastodynamics of Piezoceramic Bodies*, Springer, Cham (2021).
11. L. Grigoryeva, "Transient responses in piezoceramic multilayer actuators taking into account external viscoelastic layer," *Strength Mater. Theor. Struct.*, No. 105, 255–266 (2020).
12. L. O. Hryhorieva and I. V. Yanchevskyi, "Influence of material functional heterogeneity on non-stationary oscillations of piezoceramic bodies," *Strength Mater. Theor. Struct.*, No. 109, 359–368 (2022).
13. V. I. Kozlov, L. P. Zinchuk, and T. V. Karnaukhova, "Nonlinear vibrations and dissipative heating of laminated shells of piezoelectric viscoelastic materials with shear strains," *Int. Appl. Mech.*, **57**, No. 6, 669–686 (2021).
14. J. Li, Y. Xue, F. Li, and Y. Narita, "Active vibration control of functionally graded piezoelectric material plate," *Comp. Struct.*, No. 207, 509–518 (2019).
15. S. J. Rupitsch, *Piezoelectric Sensors and Actuators*, Springer Berlin Heidelberg, Heidelberg–Berlin (2019).
16. K. Uchino, Y. Zhuang, and S. O. Ural, "Loss determination methodology for a piezoelectric ceramic: new phenomenological theory and experimental proposals," *J. Adv. Dielect.*, **1**, No. 1, 17–31 (2011).
17. H. M. Wang, H. J. Ding, and Y. M. Chen, "Transient responses of a multilayered spherically isotropic piezoelectric hollow sphere," *Arch. Appl. Mech.*, No. 74, 581–599 (2005).
18. C. Ying and S. Zhi-fei, "Analysis of a functionally graded piezothermoelastic hollow cylinder," *J. of Zhejiang University*, *Science A*, **6,** No. 9, 956–961 (2005).